

Electronic Supplementary Information (ESI)

**Emissive nanoparticles from pyridinium-substituted
tetraphenylethylene salts: imaging and selective cytotoxicity
toward cancer cells *in vitro* and *in vivo* by varying counter
anions**

Yanyan Huang,^{a,b} Guanxin Zhang,*^{a,b} Fang Hu,^{a,b} Yulong Jin,^{a,b} Rui Zhao,*^{a,b}
Deqing Zhang*^{a,b}

^a Beijing National Laboratory for Molecular Sciences, CAS Key Laboratories of
Organic Solids and Analytical Chemistry for Living Biosystems, Institute of
Chemistry, Chinese Academy of Sciences, Beijing, 100190, China

E-mail: dqzhang@iccas.ac.cn, zhaorui@iccas.ac.cn, gxzhang@iccas.ac.cn

^b University of Chinese Academy of Sciences, Beijing 100049, China

Table of Contents

1. Experimental.....	s2
2. ¹ H- and ¹³ C-NMR spectra.....	s12
3. Scanning electron microscopy (SEM) characterization	s17
4. Absorbance and fluorescence spectra.....	s17
5. Fluorescence imaging of different cells by NanoTPES.....	s18
6. Discussion on the uptake behavior of NanoTPES 1 and NanoTPES 4 by cells..	s18
7. Monitoring the internalization of NanoTPES 2 and 3	s19
8. Co-staining experiments	s20
9. Cytotoxicity of NanoTPES towards different cells	s21
10. Estimation of the IC ₅₀ values	s21
11. Cellular uptake and cytotoxicity of 5 and 6 with different cations	s22
12. Mitochondrial damage by NanoTPES 2 and NanoTPES 3	s23
13. Evaluation of <i>in vivo</i> anti-tumor activity of NanoTPES by tumor size and H&E analysis	s25

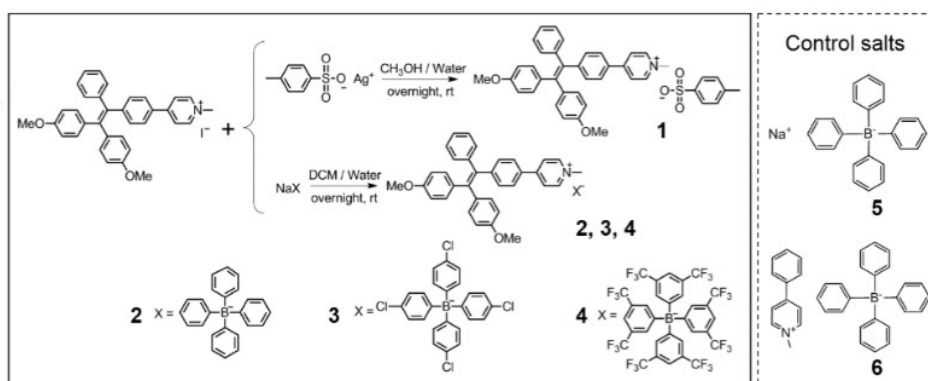
1. Experimental

Materials and characterization. Silver *p*-toluenesulfonate, sodium tetraphenyl borate (compound **5**), sodium tetra(4-chlorophenyl) borate and sodium tetra(3,5-bis(trifluoromethyl)phenyl) borate were commercial available, which were used without further purification. Dimethyl sulfoxide (DMSO) of analytical grade was from Beijing Chemical Factory (China). Dulbecco's Modified Eagle Medium (DMEM) and fetal bovine serum (FBS) were purchased from Invitrogen (California, USA). 3-(4,5-dimethylthiazol-2-yl)-2,5-diphenyltetrazolium bromide (MTT) was obtained from Sigma-Aldrich (USA). MitoTracker[®] Green FM and LysoTracker[®] Green DND-26 were from life technologies (Thermo Fisher Scientific, USA). JC-10 Mitochondria Membrane Potential Kit was purchased from Sigma-Aldrich (USA). Adenosine triphosphate (ATP) was determined with ATP Assay Kit (Beyotime, China). Hoechst 33342 was obtained from Solarbio (Beijing, China). Pyridium-substituted TPE with iodide as the counter ion and *N*-methyl-4-phenylpyridinium iodide were synthesized according to the previous work.^{S1}

Phosphate buffered saline (PBS) consisting of NaCl (137 mmol/L), KCl (2.7 mmol/L), Na₂HPO₄ (10 mmol/L) and KH₂PO₄ (2.0 mmol/L) was prepared according to the standard protocol. Ultra-pure water from a Milli-Q water purification system (Millipore, Bedford, MA) was used throughout. Other materials used for synthesis are commercial available and used as received. All solvents were purified and dried following standard procedures unless otherwise stated.

^1H NMR and ^{13}C NMR spectra were recorded on Bruker Avance 400 and 300 MHz. Fourier transform infrared (FT-IR) spectra were measured with a Tensor-27 FT-IR spectrometer (Bruker Optics, Ettlingen, Germany). Absorption spectra were recorded on a Shimadzu UV-1800 spectrometer (Japan). Fluorescence spectra were recorded on a Hitachi F-4600 spectrometer with a Xe lamp as the excitation source. Dynamic light scattering measurements were performed at 25 °C on a Zetasizer Nano ZS with a backscattering detection at 173° and a He–Ne laser (Malvern Instruments Ltd, UK). Fluorescence imaging experiments were performed on a FV 1000-IX81 CLSM (Olympus, Japan) with a UPLSAPO 100×oil-immersion objective (Olympus).

Cell culture. HepG2 cells, HeLa cells, A549 cells, HEK293 cells, Chang liver cells and L02 cells were from Shanghai Institutes for Biological Sciences, Chinese Academy of Sciences (Shanghai, China). Cells were cultured at 37 °C and 5% CO_2 in high-glucose DMEM supplemented with 10% fetal bovine serum.



Scheme S1. The chemical structures of compounds 1-6 and the synthetic approach.

Synthesis of compound 1. To a solution of the pyridium-substituted TPE with iodide as the counter ion (0.2 g, 0.33 mmol) in methanol, silver *p*-toluenesulfonate (0.11 g,

0.39 mmol) in 2 mL of deionized water was added and the mixture was stirred for 2 hours at room temperature. The solution was poured into water, extracted with dichloromethane and the organic phase was washed with brine. The organic layer was dried over anhydrous Na₂SO₄, filtered and evaporated. Then, compound **1** (0.20 g, 0.31 mmol) was obtained as an orange red solid in 96.2% yield. M.p. 164.6-165.4 °C. ¹H NMR (400 MHz, DMSO-d₆, δ): 8.93 (d, *J* = 6.8, 2H), 8.42 (d, *J* = 6.8 Hz, 2H), 7.90 (d, *J* = 8.4 Hz, 2H), 7.47 (d, *J* = 8.0 Hz, 2H), 7.19-7.09 (m, 5H), 7.10 (d, *J* = 8.0 Hz, 2H), 7.00 (d, *J* = 6.8 Hz, 2H), 6.94 (d, *J* = 8.0 Hz, 2H), 6.88 (d, *J* = 8.8, 2H), 6.75-6.70 (m, 4H), 4.23 (s, 3H), 3.68 (s, 6H), 2.28 (s, 3H); ¹³C NMR (75 MHz, CDCl₃, δ): 158.6, 158.4, 154.8, 149.0, 145.5, 143.5, 142.8, 142.4, 139.5, 137.6, 135.7, 135.6, 132.7, 131.4, 130.8, 128.8, 128.0, 127.1, 126.6, 125.9, 123.8, 113.4, 113.1, 55.1, 31.6, 21.2. FT-IR (KBr): 3436, 3053, 2955, 1642, 1603, 1507, 1462, 1293, 1247, 1178, 1034, 817, 686 cm⁻¹. Anal. calcd. for C₄₁H₃₇NO₅S·(H₂O)₃: C, 69.37; H, 6.11; N, 1.97; found: C, 69.69; H, 5.61; N, 1.95.

Synthesis of compound 2. To a solution of the pyridium-substituted TPE with iodide as the counter ion (0.23 g, 0.38 mmol) in 2 mL of CH₂Cl₂, NaBPh₄ (0.16 g, 0.46 mmol) in 1 mL of water was added. The mixture was stirred for 5 hours at room temperature. After that, the solution was poured into water, and the mixture was extracted with CH₂Cl₂. The organic layer was washed with brine and dried over sodium sulfate. After filtration and solvent evaporation, the residue was purified by silica gel column chromatography, with CH₂Cl₂/CH₃OH (20:1) as the eluent. Compound **2** (0.30 g, 0.37 mmol) was obtained as a red solid in 98.2% yield. M.p.

235.6-236.6 °C. ¹H NMR (300 MHz, DMSO-d₆, δ): 8.93 (d, *J* = 6.6, 2H), 8.42 (d, *J* = 6.6, 2H), 7.90 (d, *J* = 8.4, 2H), 7.19-7.17 (m, 13H), 7.01-6.87 (m, 14H), 6.81-6.69 (m, 8H), 4.28 (s, 3H), 3.68 (s, 6H); ¹³C NMR (75 MHz, DMSO-d₆, δ): 164.6, 164.1, 163.6, 163.1, 158.6, 158.5, 153.9, 148.6, 145.9, 143.8, 142.1, 138.0, 136.0, 135.7, 132.6, 132.51, 132.46, 131.3, 131.2, 128.6, 128.0, 127.1, 125.78, 125.75, 125.73, 125.70, 124.0, 122.0, 113.9, 113.7, 55.4, 47.4. FT-IR (KBr): 3425, 3053, 3001, 2834, 1637, 1601, 1506, 1461, 1297, 1248, 1174, 1036, 834, 737, 707 cm⁻¹. Anal. calcd. for C₅₈H₅₀BNO₂: C, 86.66; H, 6.27; N, 1.74; found: C, 86.51; H, 6.29; N, 1.84.

Synthesis of compound 3. Compound **3** was synthesized and purified similarly as for compound **2** with corresponding sodium salt. M.p. 131.9-133.5 °C. ¹H NMR (400 MHz, CD₂Cl₂, δ): 7.67 (d, *J* = 4.0, 2H), 7.59 (d, *J* = 4.0, 2H), 7.47 (d, *J* = 8.0, 2H), 7.26-7.16 (m, 13H), 7.06-6.94 (m, 14H), 6.68-6.65 (m, 4H), 3.73 (s, 6H), 3.71 (s, 3H). ¹³C NMR (100 MHz, CD₂Cl₂, δ): 161.2, 160.7, 160.2, 158.9, 158.7, 156.4, 150.4, 143.4, 137.5, 137.0, 135.5, 133.0, 132.6, 132.5, 131.3, 129.7, 128.1, 128.0, 127.2, 126.6, 125.9, 124.3, 113.3, 113.0, 55.1, 47.3. FT-IR (KBr): 3423, 3057, 3000, 2953, 2856, 1640, 1601, 1507, 1473, 1297, 1246, 1176, 1032, 833, 789, 702 cm⁻¹. Anal. calcd. for C₅₈H₄₆BCl₄NO₂: C, 73.98; H, 4.92; N, 1.49; found: C, 74.09; H, 5.53; N, 1.39.

Synthesis of compound 4. Compound **4** was synthesized and purified similarly as for compound **2** with corresponding sodium salt. M.p. 67.8-68.6 °C. ¹H NMR (300 MHz, DMSO-d₆, δ): 8.94 (d, *J* = 6.3, 2H), 8.43 (d, *J* = 6.3, 2H), 7.91 (d, *J* = 8.4, 2H), 7.39 (s, 4H), 7.62 (s, 8H), 7.20-7.17 (m, 5H), 7.01-6.87 (m, 6H), 6.76-6.70 (m, 4H), 4.23 (s,

3H), 3.69 (s, 6H); ^{13}C NMR (75 MHz, DMSO- d_6 , δ): 162.1, 161.7, 161.2, 160.7, 158.6, 158.5, 153.9, 148.6, 145.9, 143.8, 142.1, 138.0, 135.7, 134.5, 132.6, 132.51, 132.46, 131.3, 131.2, 129.4, 129.1, 128.8, 128.5, 128.0, 127.1, 125.8, 124.0, 123.1, 120.4, 118.2, 113.9, 113.7, 55.4, 47.4. FT-IR (KBr): 3433, 2930, 1640, 1603, 1509, 1465, 1356, 1279, 1248, 1176, 1127, 1034, 836, 713 cm^{-1} . Anal. calcd. for $\text{C}_{66}\text{H}_{42}\text{BF}_{24}\text{NO}_2$: C, 58.81; H, 3.14; N, 1.04; found: C, 59.31; H, 3.43; N, 1.02.

Synthesis of compound 6. Compound **6** was synthesized from *N*-methyl-4-phenylpyridinium iodide and sodium tetraphenyl borate (compound **5**). To a solution of *N*-methyl-4-phenylpyridinium iodide (0.26 g, 0.87 mmol) in 2.0 mL of CH_2Cl_2 , NaBPh_4 (0.36 g, 1.04 mmol) in 1.0 mL of water was added. The mixture was stirred for 5 hours at room temperature. After that, the solution was poured into water, and the mixture was extracted with CH_2Cl_2 . The organic layer was washed with brine and dried over sodium sulfate. After filtration and solvent evaporation, the residue was purified by silica gel column chromatography, with $\text{CH}_2\text{Cl}_2/\text{CH}_3\text{OH}$ (20:1) as the eluent. Compound **6** (0.42 g, 0.86 mmol) was obtained as a white solid in 99.1% yield. M.p. 222.8-223.3 $^\circ\text{C}$. ^1H NMR (400 MHz, DMSO- d_6 , δ): 9.00 (d, $J = 6.8$, 2H), 8.50 (d, $J = 6.8$, 2H), 8.07 (d, $J = 7.8$, 2H), 7.66-7.65 (m, 3H), 7.17 (m, 8H), 6.94-6.90 (m, 8H), 6.80-6.78 (m, 4H), 4.33 (s, 3H); ^{13}C NMR (100 MHz, DMSO- d_6 , δ): 164.6, 164.1, 163.6, 163.1, 154.8, 146.1, 136.0, 134.0, 132.5, 130.2, 128.5, 125.79, 125.77, 125.74, 125.71, 124.6, 122.0, 47.5. FT-IR (KBr): 3424, 3053, 3001, 1641, 1579, 1480, 1431, 1267, 847, 737, 708 cm^{-1} . Anal. calcd. for $\text{C}_{36}\text{H}_{32}\text{BN}$: C 88.34; H 6.59; N 2.86; found: C 88.29; H 6.58; N 2.94.

Preparation of nanoparticles and characterization. A DMSO solution (10 μL , 2 mM) of respective compounds (**1-4**) was added to a PBS (990 μL) solution. After shaken for 30 s, the solutions were kept in dark for further test. The size of nanoparticles was characterized with DLS and SEM.

Absorbance and fluorescence spectroscopy. Absorption spectra were recorded on a Shimadzu UV-1800 spectrometer (Japan). Fluorescence spectra were recorded on a Hitachi F-4600 spectrometer with a Xe lamp as the excitation source. Typically, stock solution of each compound was prepared in DMSO to a concentration of 2 mM. For measurement, 10 μL stock solution was diluted with PBS to a final volume of 1.0 mL. The corresponding fluorescence spectrum was recorded with 405 nm excitation, and the emission was collected from 450 to 800 nm.

The fluorescence quantum yields of NanoTPES **1-4** in PBS solutions containing 1% DMSO were measured with FLSP 920 fluorescence spectrometer containing a calibrated integrating sphere system. The measurements were carried out at room temperature.

Cell imaging. In 35 mm glass-bottomed dishes, the cells (approximately $1.0 \times 10^5/\text{mL}$) were seeded and cultured overnight for adhesion. After carefully washed with PBS for three times, the cells were treated with NanoTPES solution (500 μL , 20 μM). After incubation, the cells were subjected to imaging analysis after washed with PBS once. Fluorescence imaging experiments were performed on a FV 1000-IX81 CLSM (Olympus, Japan). The objective used for imaging was a UPLSAPO 100 \times oil-

immersion objective (Olympus). Image processing and analysis were performed on Olympus software (FV10-ASW). Nanoparticles were excited by a 50 mW, 405 nm Laser Head FV5-LD405-2. For NanoTPES **1**, the fluorescence was collected with a band-pass filter within the range of 500–600 nm. For NanoTPES **2**, NanoTPES **3** and NanoTPES **4**, the fluorescence was collected with a band-pass filter within the range of 550–650 nm.

For co-staining assay, the NanoTPES **2**- and NanoTPES **3**-loaded HepG2 cells were subjected for the incubation with MitoTracker, LysoTracker, or Hoechst 33342 solutions respectively. After washed with PBS, the cell samples were observed with CLSM. NanoTPES **2** and **3** were excited by a 50 mW, 405 nm Laser Head FV5-LD405-2 and collected with a band-pass filter within the range of 580–680 nm. For MitoTracker and LysoTracker, an FV5-LAMAR 488 nm laser was used as the excitation source. Their green fluorescence was collected with a band-pass filter within the range of 500–550 nm. Hoechst 33342 was excited by a 50 mW, 405 nm Laser Head FV5-LD405-2 and collected with a band-pass filter within the range of 425–475 nm.

Flow-cytometric analysis. The uptake of NanoTPES **2** and **3** by HepG2 cells was also determined by flow cytometric analysis. After incubated with NanoTPES **2** or **3** for 60 min, HepG2 cells were washed with PBS, and then re-suspended. The fluorescence of the stained cells (3×10^4) was recorded with a BD accuri C6 flow cytometer (BD Biosciences, USA). The dependence of fluorescence intensity on the concentration of NanoTPES was analyzed using Sigma Plot (Jandel, San Rafael, CA).

MTT assay. The viability of different cells was evaluated by the standard MTT assay. Cells (100 μL) were seeded to 96-well plate at a density of 5×10^4 /mL. After 24-hour incubation, the culture medium was replaced by NanoTPES solutions. The cells were further cultured at 37 $^{\circ}\text{C}$ for another 48 hours. Then, the culture medium was carefully removed, and 100 μL of freshly prepared MTT solution (0.5 mg mL^{-1} in culture medium) was added into each well. After incubation at 37 $^{\circ}\text{C}$ for 4 hours, the MTT solution was removed and 150 μL DMSO was added to dissolve the formazan crystals. The plate was shaken for 10 min to fully dissolve formazan and homogenize. Absorbance values of the wells were read with a microplate reader at 570 nm (BIO RAD, iMark). The cell viability rate (VR) was calculated from the following equation: $\text{VR} = A/A_0 \times 100\%$, where A is the absorbance of the experimental group and A_0 is the absorbance from the cells cultured in serum-supplemented medium without any treatment. All data were obtained from three repeatedly parallel experiments.

Mitochondrial membrane potential assay and ATP assay. CLSM and microplate assay were used for investigating the mitochondrial membrane potential ($\Delta\Psi_m$) in cells. After treated with NanoTPES **2** and **3** for 2 hours, the media containing NanoTPES was removed. The cells were washed with PBS and then incubated with JC-10 dye for 30 min. After washed with PBS for three times, the cells were observed with CLSM. The green fluorescence from JC-10 monomer was excited with a FV5-LAMAR 488 nm laser, and collected with a band-pass filter within the range of 500–545 nm. The red fluorescence of J -aggregates was excited with a 559-nm laser, and collected within the range of 570–670 nm. For microplate assay, the cells were seeded

at a density of 60000 cells/well (90 μ L). After 24 hours, NanoTPES **2** and **3** solutions were spiked into the culture media (final concentration: 20 μ M). After a further culture for 2 hours, JC-10 loading solution of 50 μ L was added to each well and the treatment was lasted for 30 min. The fluorescence intensities (green: $\lambda_{\text{ex.}}$ = 490 nm, $\lambda_{\text{em.}}$ = 525 nm; red: $\lambda_{\text{ex.}}$ = 540 nm, $\lambda_{\text{em.}}$ = 590 nm) were recorded with PerkinElmer EnSpire Multimode Plate Reader (USA). The ratio of red/green fluorescence intensity is used to determine $\Delta\Psi_{\text{m}}$.

The ATP content was determined with an ATP assay Kit (Beyotime) according to the manufacturer's instruction. Typically, HepG2 cells were seeded in 6-well plates. After adhesion, cells were treated with NanoTPES **2** or **3** (20 μ M) for 2 hours. Then, the media containing NanoTPES was removed. The cells were lysed with the cell lysis solution (200 μ L), and the lysates were collected for centrifugation (4 $^{\circ}$ C, 12000 rpm). In a test tube, the ATP-testing solution (200 μ L) was added in advance. After 5.0 min, the supernatant of the cell lysates (100 μ L) was added and mixed with the ATP-testing solution. The luminescence was recorded immediately. For the control experiments, HepG2 cells were treated with the same procedures except the incubation with NanoTPES.

***In vivo* antitumor study.** Female BALB/c nude mice (5–6 weeks) were purchased from Vital River Laboratories (Beijing, China). All animal experiments were performed in accordance with the Guide for the Care and Use of Laboratory Animals, and were approved by the Experimental Animal Ethics Committee in Beijing. Mice were subcutaneously injected with HepG2 cells (3×10^7 /mL, 200 μ L) at the flank.

After the tumor grew to a volume of $\sim 60 \text{ mm}^3$, the mice were randomly divided to three groups, with five mice in each group. The tumor-bearing mice in the three groups were treated with PBS (1% DMSO), NanoTPES **2** and **3** respectively every other day. The dosage of NanoTPES **2** and **3** was 1.7 mg/kg. Tumor volume were measured and calculated by Tumor volume = (length \times width²)/2. On day 20, mice were euthanized. The tumor tissue, heart, liver, spleen, lung and kidney of each mice were collected and fixed in formalin. Hematoxylin and eosin staining of the tissues was performed according to standard protocol.

***In vivo* optical imaging.** The tumor-bearing mice were injected intravenously via tail vein with either PBS (1% DMSO) or NanoTPES (1.7 mg/kg). After 60 min, mice were anesthetized and imaged with a small animal *in vivo* imaging system CRI Maestro 2 (Cambridge Research & Instrumentation, Inc., USA). The emission was collected from 630 nm to 800 nm (9 s exposure). After imaging, the mice were sacrificed. Tumor, heart, liver, spleen, lung and kidney were removed and imaged under the same condition to access the distribution of the NanoTPES. The images were analyzed with Maestro2 software.

2. ¹H- and ¹³C-NMR spectra

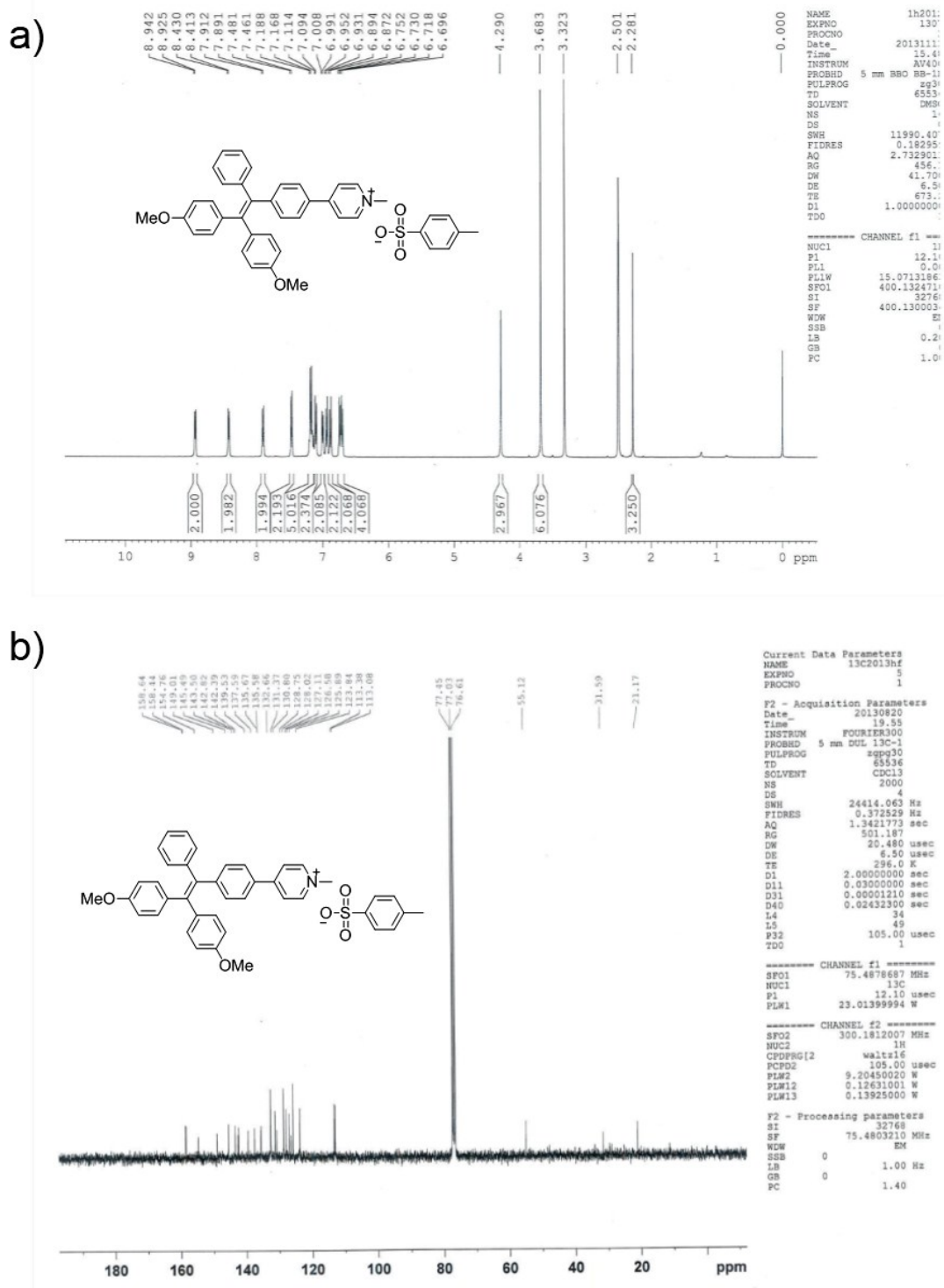
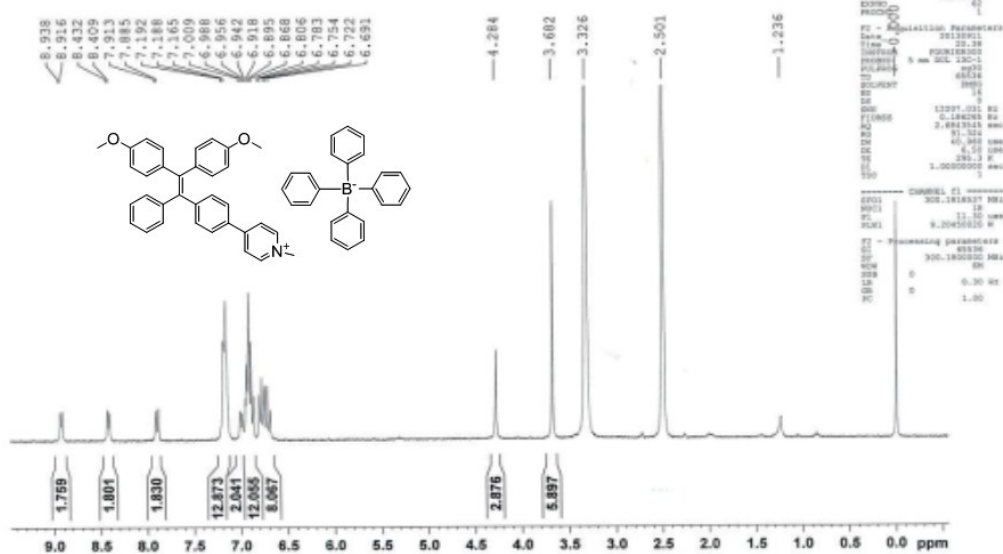


Figure S1. (a) ¹H-NMR spectrum of compound **1** in DMSO-*d*₆; (b) ¹³C-NMR spectrum of compound **1** in CDCl₃.

a)



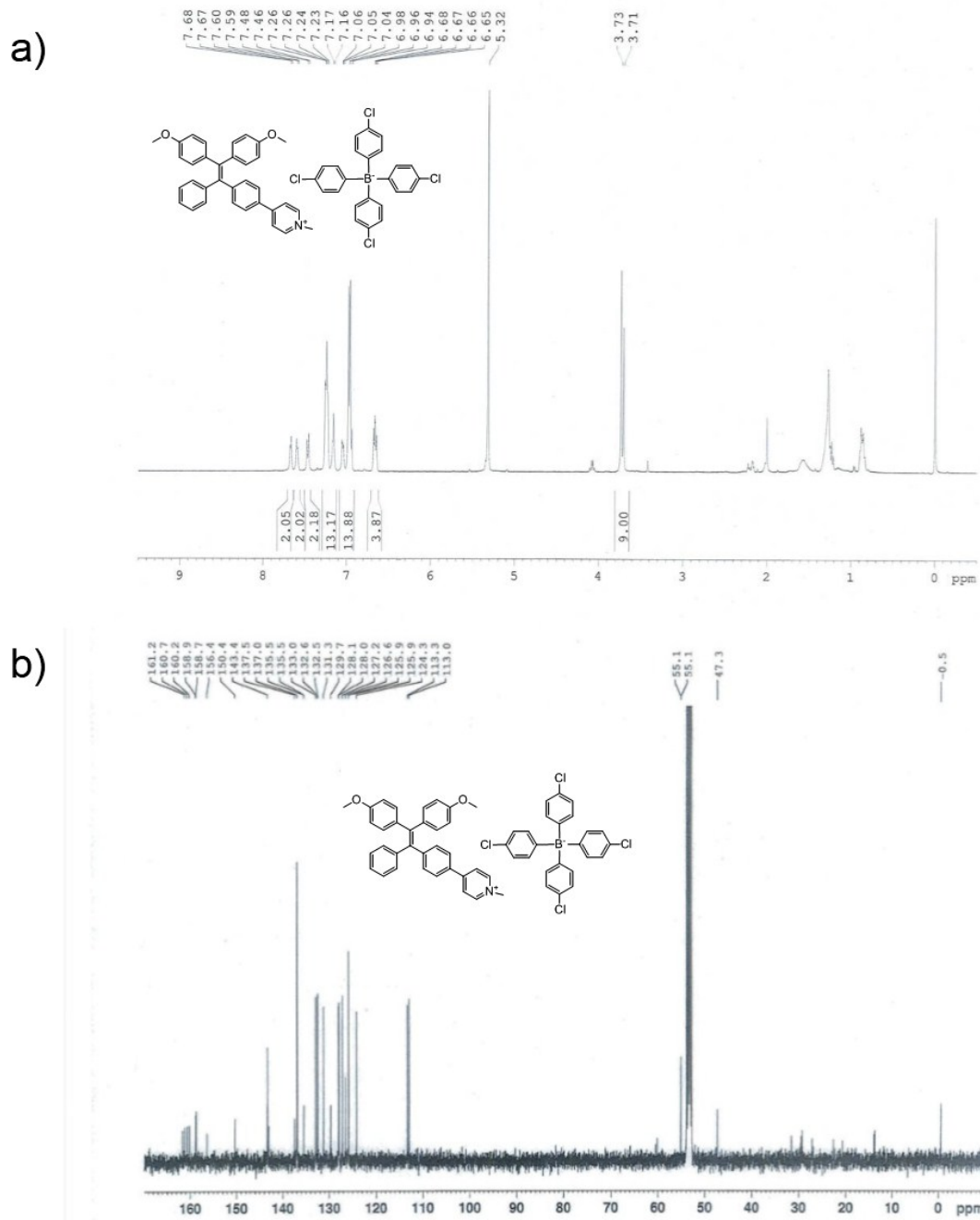


Figure S3. (a) ^1H -NMR spectrum of compound **3** in CD_2Cl_2 ; (b) ^{13}C -NMR spectrum of compound **3** in CD_2Cl_2 .

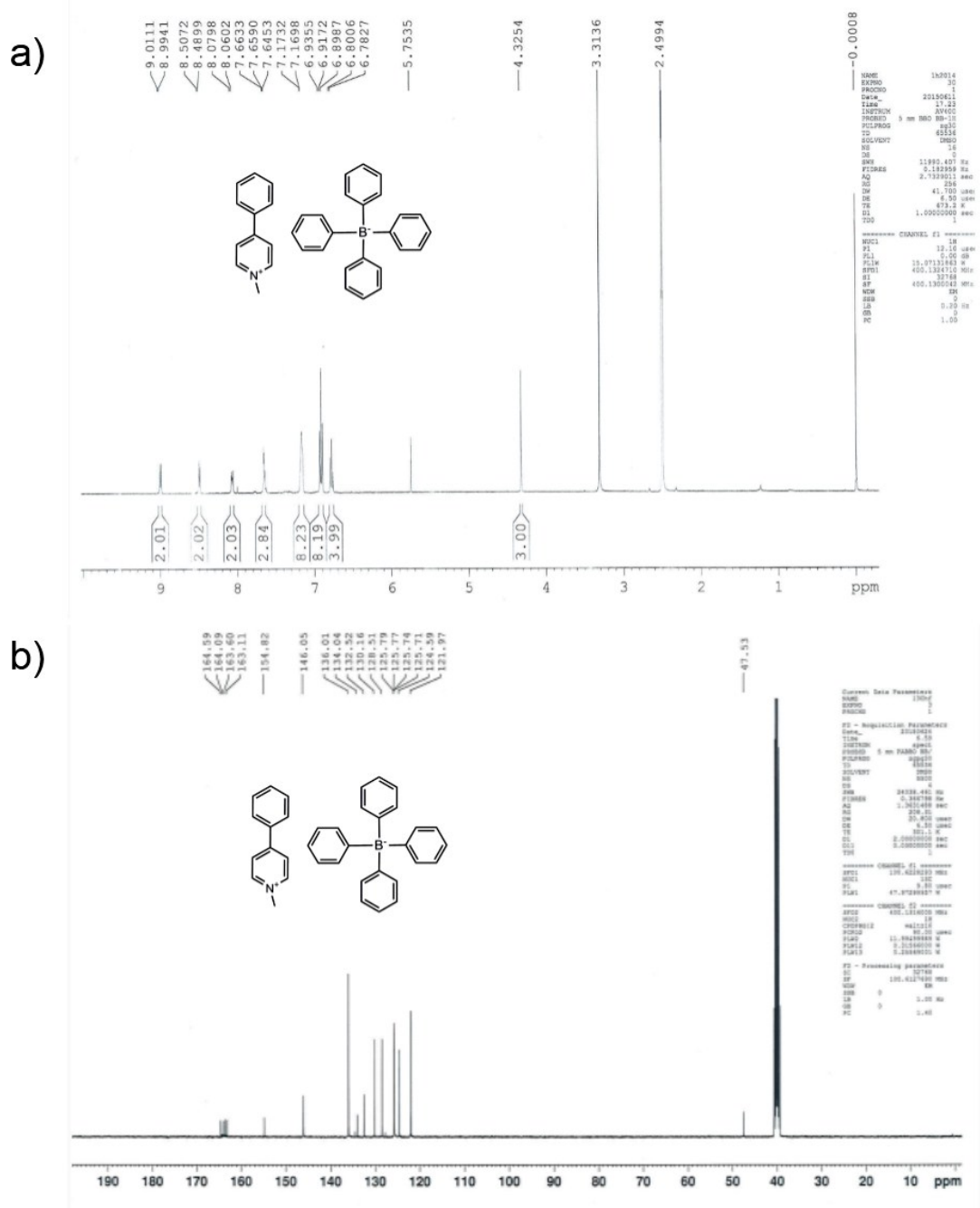


Figure S5. (a) ^1H -NMR spectrum of compound **6** in $\text{DMSO-}d_6$; (b) ^{13}C -NMR spectrum of compound **6** in $\text{DMSO-}d_6$.

3. Scanning electron microscopy (SEM) characterization

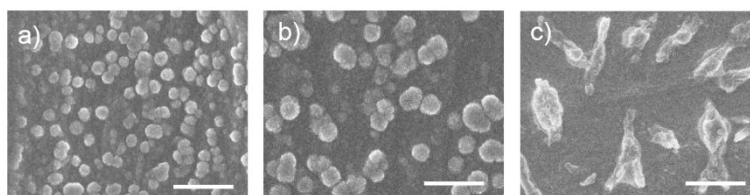


Figure S6. SEM characterization of NanoTPES. (a) NanoTPES 1, (b) NanoTPES 3, (c) NanoTPES 4; scale bar: 500 nm.

4. Absorbance and fluorescence spectra

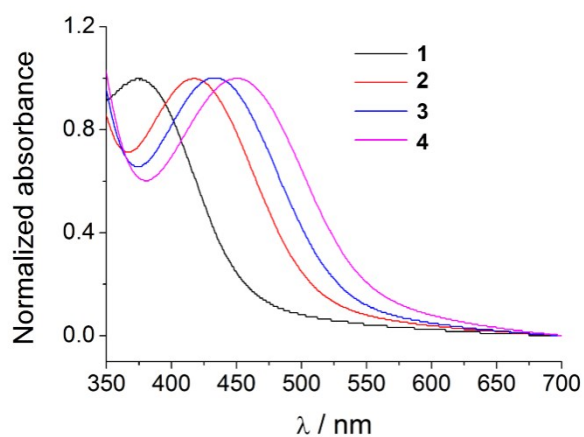


Figure S7. Absorption spectra of NanoTPES 1-4 (20 μM) in PBS containing 1% DMSO.

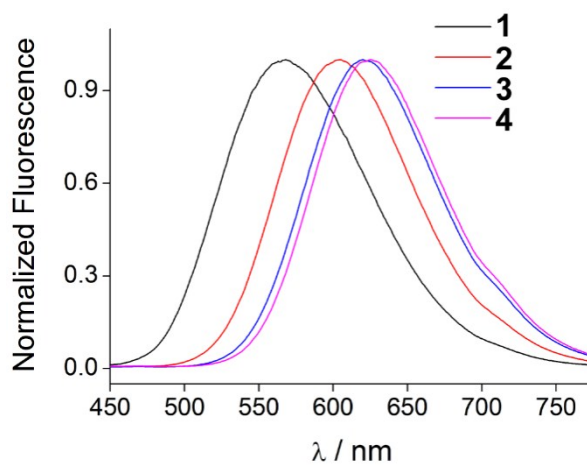


Figure S8. Fluorescence emission spectra of NanoTPES 1-4 (20 μM) in PBS containing 1% DMSO.

5. Fluorescence imaging of different cells by NanoTPES

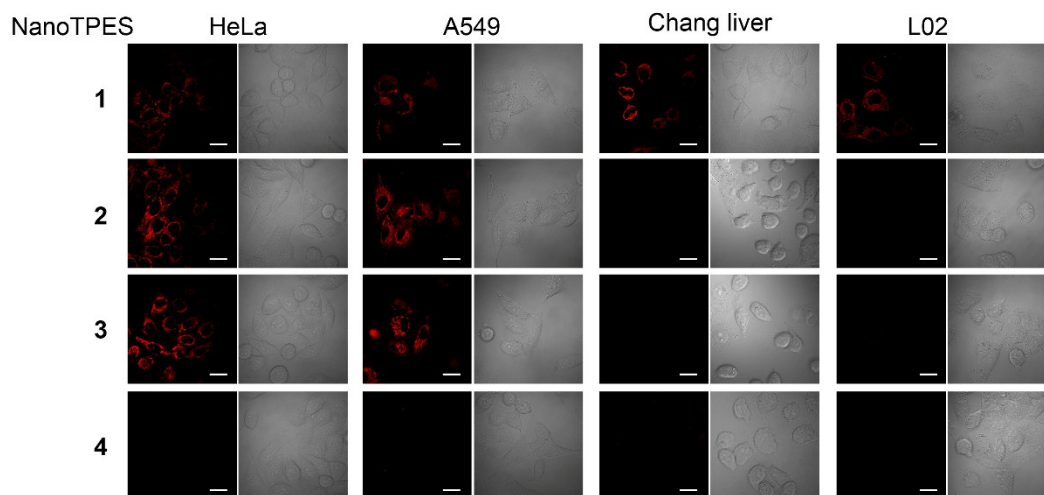


Figure S9. CLSM images of cancer cells (HeLa and A549 cells) and normal cells (Chang liver and L02 cells) after incubation with NanoTPES 1-4 (20 μ M), respectively; the scale bar is 20 μ m.

6. Discussion on the uptake behavior of NanoTPES 1 and NanoTPES 4 by cells

As listed in Table 1 the surface zeta-potential of NanoTPES 1 is approximately neutral (just slightly positive), but the average size is much smaller than those of NanoTPES 2 and NanoTPES 3. Thus, hydrophobic interactions may play an important role in the interaction of NanoTPES 1 with cell membrane. Because of its small size, NanoTPES 1 should be easier to be uptaken by both HepG2 and HEK293 cells.^{s2} For NanoTPES 4, however, the surface zeta-potential becomes negative and as a result the electrostatic repulsion will retard its interaction with both cancer and normal cells. Additionally, the average size of NanoTPES 4 is rather larger (Table1) which will further prevent its entrance into cells.

7. Monitoring the internalization of NanoTPES 2 and 3

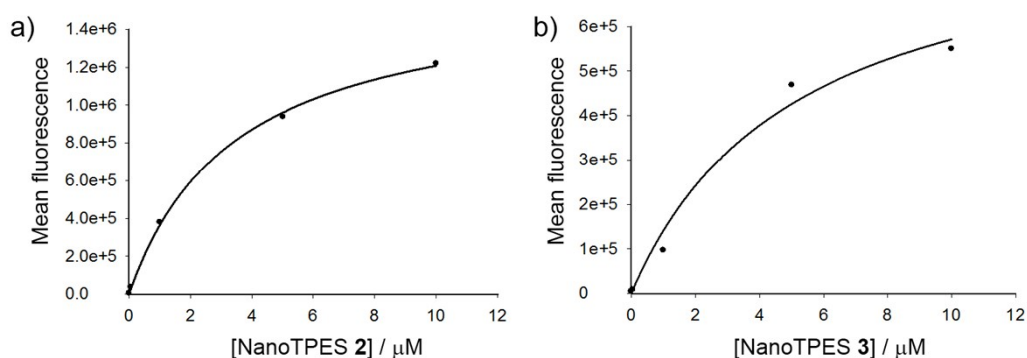


Figure S10. Flow cytometry to determine the specific uptake behavior of NanoTPES 2 (a) and NanoTPES 3 (b) towards HepG2 cells.

A time-course fluorescence assay was carried out to monitor the intracellular trafficking of NanoTPES. The red fluorescence from NanoTPES 2 initially showed a dotted distribution on the cell membrane, which further intensified to cover the whole membrane with 20-min incubation (Figure S11). After 30 min, the red fluorescence inside HepG2 cells appeared and increased, suggesting the entrance of NanoTPES 2 into cytoplasm. With another 30 min, a very clear target-to-background image was acquired indicating the completion of subcellular localization (Figure S11).

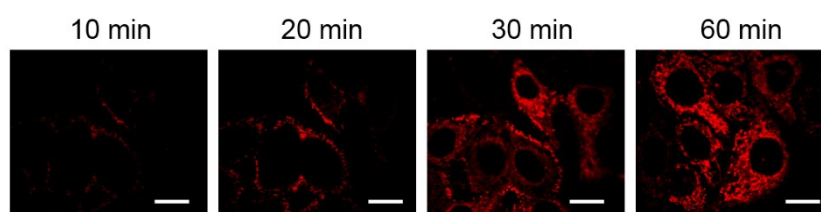


Figure S11. Monitoring the internalization of NanoTPES 2 to HepG2 cells at different incubation time, scale bar: 20 μm .

8. Co-staining experiments

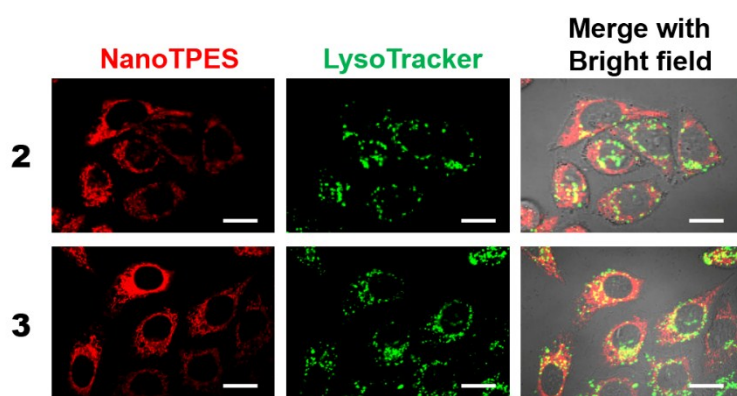


Figure S12. Co-staining of NanoTPES **2** and **3** (20 μ M) with lysosomal tracker Green in HepG2 cells; scale bar: 20 μ m.

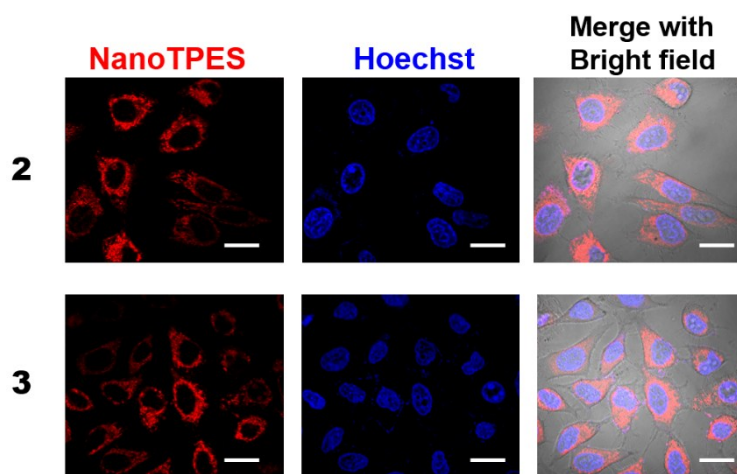


Figure S13. Co-staining of NanoTPES **2** and **3** (20 μ M) with Hoechst33342 in HepG2 cells; scale bar: 20 μ m.

9. Cytotoxicity of NanoTPES towards different cells

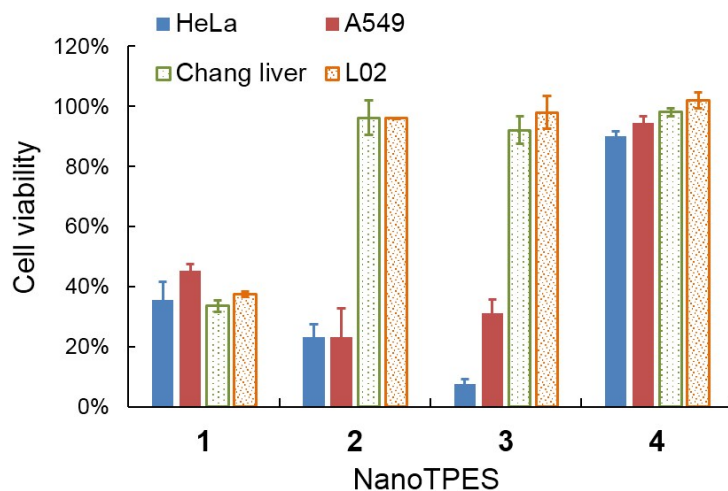


Figure S14. Cell viabilities of HeLa, A549, Chang liver and L02 cells after treated with NanoTPES 1-4 (10 μ M) for 48 hours.

10. Estimation of the IC_{50} values

Different concentrations of NanoTPES 2 and NanoTPES 3 were examined for the ablation of HepG2 cells. On the basis of the cell viability data (Figures S15), the IC_{50} values of NanoTPES 2 and NanoTPES 3 towards HepG2 cells were estimated to be 2.2 μ M and 3.8 μ M, respectively.

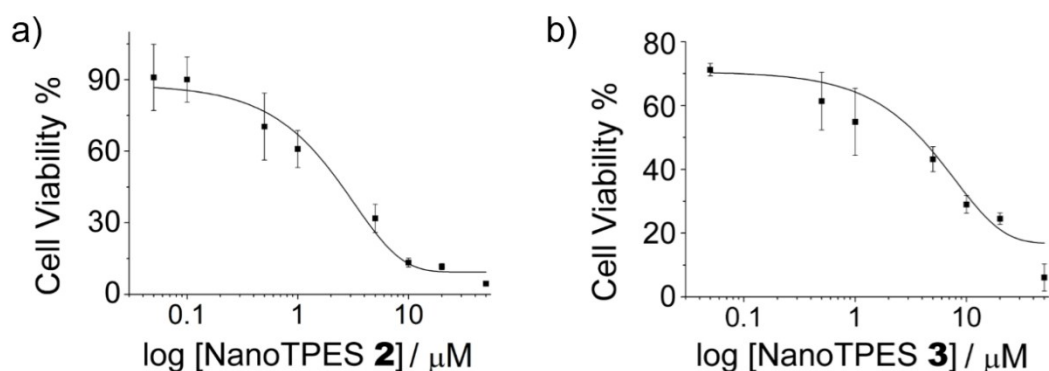


Figure S15. Variation of cell viability for HepG2 cells vs. the concentration of NanoTPES 2 (a) and NanoTPES 3 (b), respectively.

11. Cellular uptake and cytotoxicity of 5 and 6 with different cations

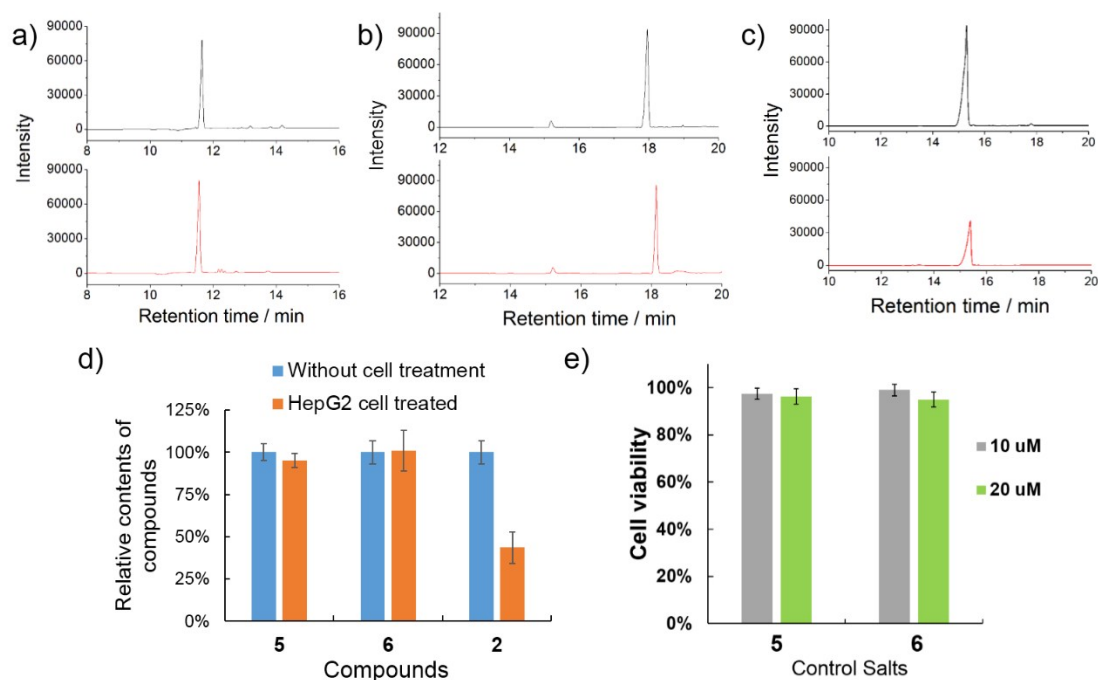


Figure S16. HPLC analysis of the solutions of **5** (a), **6** (b) and **2** (c) before (up, black line) and after (below, red line) incubations with HepG2 cells; the concentration of each solution was 20 μM ; variation of the concentrations of **5**, **6** and **2** before and after the respective incubations with HepG2 cells (d); cell viability HepG2 cells after the respective treatments with **5** and **6** (e).

The possible cellular uptake of **5** and **6** was examined with HPLC by monitoring the variation of concentrations of their supernatant solutions after the respective incubations with HepG2 cells. The experiments were carried out as follows: HepG2 cells were seeded in the 6-well plates (approximately $1.0 \times 10^5/\text{mL}$) and cultured overnight for adhesion. After being carefully washed with PBS for three times, the cells were incubated with solutions of **5** (20 μM) and **6** (20 μM), respectively. After incubation for 2.0 hours, the supernatant solution (500 μL) in each well was collected and subjected for HPLC analysis. For comparison, 500 μL of solutions of **5** (20 μM) and **6** (20 μM) without incubations with HepG2 cells were also analyzed by HPLC.

By integrating the respective peak areas in the chromatograms, the variation of concentration for **5** and **6** after cell incubation was estimated. For comparison, the experiments were also performed with solution of **2** under the same condition.

As depicted in Fig. S16 (d), the variations of the concentrations of **5** and **6** before and after incubations with HepG2 cells were negligible. In comparison, the concentration of **2** was reduced by 56% after incubation with HepG2 cells, being in agreement with cellular uptake of **2** on the basis of CLSM and flow-cytometric results. Therefore, it can be concluded that the uptake of either **5** or **6** by HepG2 cells can be neglected.

12. Mitochondrial damage by NanoTPES 2 and NanoTPES 3

Mitochondrial membrane potential ($\Delta\Psi_m$) was measured with a commercial JC-10 dye on the basis i) it shows red fluorescence upon aggregation in healthy negatively charged mitochondria, and ii) it becomes green emissive when $\Delta\Psi_m$ is reduced and mitochondria is damaged. As depicted in Figure S17a, red fluorescence was observed for polarized mitochondria in HepG2 cells without treatment. However, after incubation with NanoTPES **2** for 60 min. the red fluorescence became weak, and the green fluorescence emerged simultaneously, indicating the reduction of $\Delta\Psi_m$. After extension of the incubation to 90 min, the red fluorescence almost disappeared, whereas the green fluorescence was further enhanced. These results reveal that dramatic damages occurred to mitochondria of HepG2 cells after treatment with NanoTPES **2**. For quantitative estimation, microplate assay was carried out by calculating the ratios of the red and green fluorescence intensities. As shown in Figure

S17b, the intensity ratio decreased by 90% after incubation with NanoTPES **2**. Similarly, the intensity ratio was reduced by 88% after incubation with NanoTPES **3**. These results hint that the selective cytotoxicity of NanoTPES **2** and NanoTPES **3** toward HepG2 cells may be operated via the mitochondria damage-mediated cell apoptosis pathway.

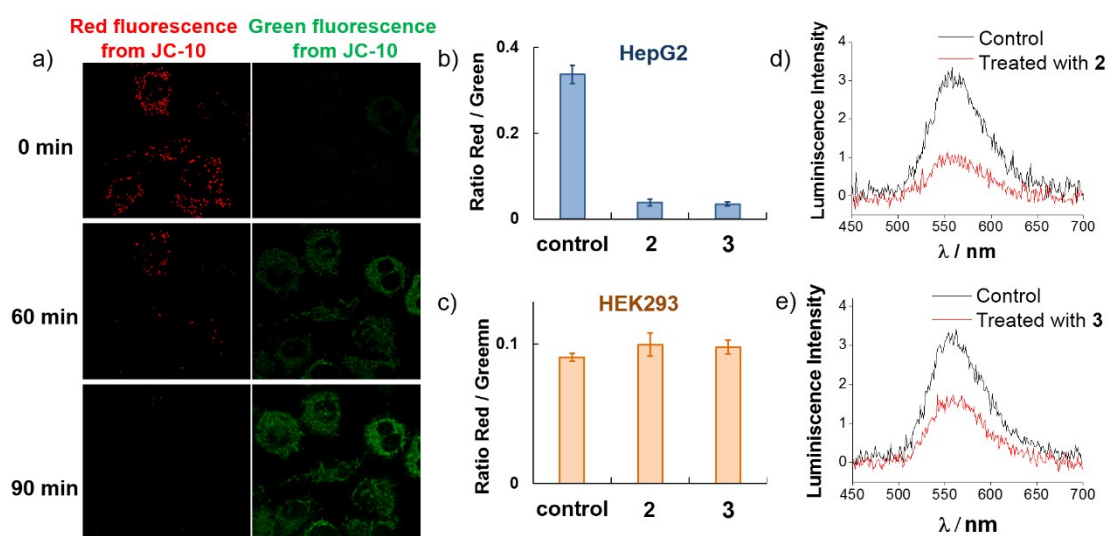


Figure S17. (a) Monitoring mitochondrial membrane potential ($\Delta\Psi_m$) of HepG2 cells with JC-10 kit after treated with NanoTPES **2** (20 μ M) for different incubation time; (b, c) Estimation of the $\Delta\Psi_m$ loss in HepG2 cells and HEK293 cells after treated with NanoTPES **2** and NanoTPES **3** for 2 hours, respectively; (d, e) Comparison of ATP contents in HepG2 cells with and without the treatment of NanoTPES **2** and NanoTPES **3** for 2 hours, respectively.

One major function of mitochondria is the production of adenosine triphosphate (ATP). To examine the functionality of mitochondria during NanoTPES treatment, the ATP content in HepG2 cells with and without the treatment of NanoTPES was measured by using an ATP bioluminescent assay kit. By calculating the relative luminescent intensities, the amounts of ATP generated in HepG2 cells after incubations with NanoTPES **2** and NanoTPES **3** decreased by 67% and 57% of that

before the treatments (Figure S17d, S17e). These results can lead to the conclusion that NanoTPES **2** and NanoTPES **3** can inhibit the oxidative phosphorylation process in mitochondria, thus the ATP supply in HepG2 cells is reduced, which will result in the death of HepG2 cells.

13. Evaluation of *in vivo* anti-tumor activity of NanoTPES by tumor size and H&E analysis

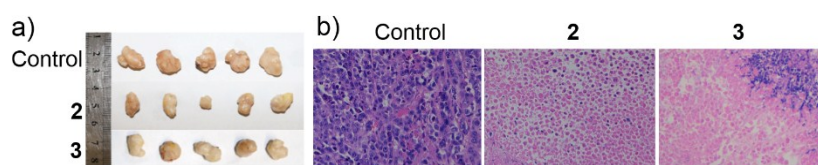


Figure S18. (a) Photographs of the tumor after intratumor injection of PBS (1% DMSO), NanoTPES **2** and **3** for 20 days, respectively; (b) H&E analysis of tumor tissues from mice intratumorally injected with PBS containing 1% DMSO, NanoTPES **2** and **3** for 20 days, respectively.

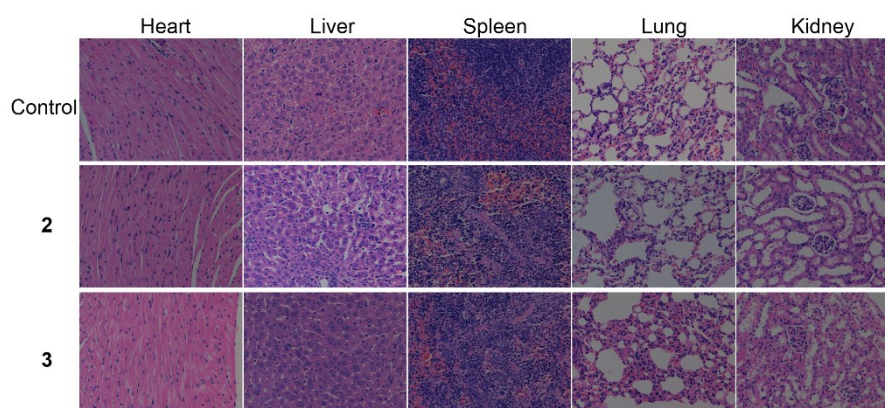


Figure S19. Evaluation of the side effect of intravenous injection of NanoTPES to tumor-bearing mice. H&E analysis of tissues from different organs in mice after intravenously injected with PBS containing 1% DMSO, NanoTPES **2** and NanoTPES **3** for 20 days, respectively.

References

- S1 F. Hu, G. Zhang, C. Zhan, W. Zhang, Y. Yan, Y. Zhao, H. Fu and D. Zhang, *Small*, 2015, **11**, 1335.
- S2 M. E. Davis, Z. G. Chen and D. M. Shin, *Nat. Rev. Drug Discovery*, 2008, **7**, 771.